

SLAC-PUB-9922
 BABAR-PROC-03-011
 June 2003

RECENT RESULTS ON $|V_{ub}|$, $|V_{cb}|$ AND MIXING FROM BABAR

D. del Re

(representing the BABAR Collaboration)

Università di Fisica “La Sapienza”, Dipartimento di Fisica, P.le Aldo Moro 2, Rome, Italy

and

University of California, San Diego, Department of Physics, La Jolla, CA 92093, USA



We present the measurements of the CKM matrix parameters V_{ub} , V_{cb} and of the B mixing oscillation frequency with the BABAR experiment at the asymmetric B -factory PEP-II. Data were collected in the years 2000-2002 and the total available statistics corresponds to 91 fb^{-1} . The V_{ub} , V_{cb} measurements utilize both inclusive and exclusive semileptonic decays of the B meson. The Δm_d parameter is measured by using the time evolution of the B , determined from the flight length difference between the two B mesons.

1 Introduction

Precise measurements of the matrix elements $|V_{ub}|$ and $|V_{cb}|$ and the mixing Δm_d parameter allow to perform tests of the unitarity of Cabibbo-Kobayashi-Maskawa (CKM) matrix¹. In this paper I present a measurement of $|V_{ub}|$ using inclusive semileptonic B decays. The analysis is based on $B\bar{B}$ events in which one of the B mesons decays hadronically and is fully reconstructed (B_{reco}) and the semileptonic decay of the recoiling B meson (B_{recoil}) is detected by a charged lepton. To separate the signal decays $\bar{B} \rightarrow X_u \ell \bar{\nu}$ from the background we use the invariant mass m_X of the hadronic system recoiling against the charged lepton and the neutrino. Moreover I present a measurement of the exclusive semileptonic branching ratio $\mathcal{B}(B^0 \rightarrow D^{*-} \ell^+ \nu_\ell)$. This channel is of particular physical interest, since the study of its differential decay rate can be used to measure the element $|V_{cb}|$. Finally the sample of $B^0 \rightarrow D^{*-} \ell^+ \nu_\ell$ decays has been also used to extract the Δm_d mixing parameter.

1.1 The Dataset and the *BABAR* Experiment

These measurements are based on data recorded by the *BABAR* detector² at the PEP-II asymmetric-energy e^+e^- storage ring at SLAC. The data sample of about 88 million $B\bar{B}$ pairs corresponds to an integrated luminosity of 81.9 fb^{-1} collected at the $\Upsilon(4S)$ resonance. The *BABAR* detector consists of a five-layer silicon vertex tracker (SVT), a 40-layer drift chamber (DCH), a detector of internally reflected Cherenkov light (DIRC), an electromagnetic calorimeter (EMC), assembled from 6580 CsI(Tl) crystals, all embedded in a solenoidal magnetic field of 1.5 T and surrounded by an instrumented flux return (IFR).

2 Measurement of the Inclusive Charmless Semileptonic Branching Fraction of B Mesons and Determination of $|V_{ub}|$

2.1 Signal Simulation

In charmless semileptonic decays, we expect resonant states to dominate at low recoil masses, while at high mass we expect non-resonant multi-hadron states to prevail. Consequently, we choose to employ a hybrid model. We use the ISGW2 model³ to produce the pseudo-scalar, vector, and heavier mesons to represent 25%, 35%, and 40%, of the resonant states, respectively; this is consistent with currently measured branching fractions⁴. We add a non-resonant component on the basis of HQET and OPE calculations⁵, where the fragmentation is handled by JETSET⁶. The two components are combined so that the inclusive charmless semileptonic branching fraction is compatible with this measurement and the LEP average and so that the integral distribution function is consistent with the OPE calculation, except for discontinuities (due to resonances) at the lowest masses. The non-resonant component amounts to about 66% of the total charmless semileptonic branching fraction. The motion of the b quark inside the B meson is implemented with the parametrization described in⁵.

2.2 Selection of Hadronic B Decays, $B \rightarrow \bar{D}Y$

This analysis is based on $B\bar{B}$ events in which one of the B mesons decays hadronically. Hadronic B decays of the type $B \rightarrow \bar{D}Y$ are selected, where D refers to a charm meson, and Y represents a collection of hadrons with a total charge of ± 1 , composed of $n_1\pi^\pm + n_2K^\pm + n_3K_S^0 + n_4\pi^0$, where $n_1 + n_2 < 6$, $n_3 < 3$, and $n_4 < 3$. Using D^- and D^{*-} (\bar{D}^0 and \bar{D}^{*0}) as seeds for B^0 (B^+) decays, we reconstruct about 1000 different decay chains. The efficiency to reconstruct a hadronic B decay amounts to 0.15% for B^0 mesons and to 0.25% for B^+ mesons.

The kinematic consistency of a B_{reco} candidate with a B meson decay is checked using two variables, the beam energy-substituted mass $m_{\text{ES}} = \sqrt{s/4 - \vec{p}_B^2}$ and the energy difference, $\Delta E = E_B - \sqrt{s}/2$. Here \sqrt{s} refers to the total energy in the $\Upsilon(4S)$ center of mass frame, and p_B and E_B denote the momentum and energy of the B_{reco} candidate in the same frame, respectively. We require $\Delta E = 0$ within approximately three standard deviations.

2.3 Selection of Semileptonic Decays, $\bar{B} \rightarrow X\ell\bar{\nu}$

Semileptonic B decays are identified by the presence of an electron or muon candidate. To reduce backgrounds from secondary charm or τ^\pm decays and from fake leptons, we only retain events with a charged lepton with a minimum momentum in the B rest frame of $p_\ell^* > 1\text{ GeV}/c$. The details of both the lepton identifications are described elsewhere².

To further improve this rejection, we require that the lepton charge and the flavor of the reconstructed B^\pm are consistent with a prompt semileptonic decay of the B_{recoil} . For B^0 we

do not impose this restriction, instead we take into account B^0 - \bar{B}^0 mixing and correct for the contribution from secondary leptons.

2.4 Selection of $\bar{B} \rightarrow X_u \ell \bar{\nu}$ Decays

The hadron system X in the decay $\bar{B} \rightarrow X \ell \bar{\nu}$ is constituted from charged tracks (excluding leptons with $p^* > 1 \text{ GeV}/c$), photons, and K^0 that are not associated with the B_{reco} candidate. Specifically, we select charged tracks in the fiducial volume $0.41 < \theta_{\text{lab}} < 2.54 \text{ rad}$. Photons are identified as energy clusters in the EMC that are spatially separated from any charged track, have an energy $E_{\text{lab}} > 80 \text{ MeV}$, and have a lateral cluster shape consistent with a photon. Care is taken to eliminate duplicate, curling, and fake charged tracks, as well as low energy photons from beam background and energy depositions in the EMC by charged and neutral hadrons.

We improve the resolution in the measurement of m_X with a 2-C kinematic fit that imposes four-momentum conservation, the equality of the masses of the two B mesons and forces $p_{\bar{\nu}}^2 = 0$.

The selection of $\bar{B} \rightarrow X_u \ell \bar{\nu}$ decays is tightened by requiring (1) one and only one charged lepton with $p_{\ell}^* > 1 \text{ GeV}/c$ in the event, (2) charge conservation, *i.e.*, the total charge of the B_{reco} , electron and the hadron system is required to be $Q_{\text{tot}} = 0$; and (3) for the missing mass of the event, $m_{\text{miss}}^2 < 0.5 \text{ GeV}^2/c^4$. These criteria not only improve the resolution in the measurement of the missing neutrino, they also suppress the dominant $\bar{B} \rightarrow X_c \ell \bar{\nu}$ decays, many of which contain additional neutrinos or undetected K_L .

To further suppress $\bar{B}^0 \rightarrow D^{*+} \ell^- \bar{\nu}$ decays, we exploit the fact that the momentum of the pion produced in the $D^{*+} \rightarrow D^0 \pi^+$ decay is almost collinear with the D^{*+} momentum in the laboratory frame. In that frame we can approximate the energy of the D^{*+} as $E_{D^{*+}} \simeq \gamma m_{D^{*+}} = E_{\pi} \cdot m_{D^{*+}}/145 \text{ MeV}$ and then require for the mass of the neutrino $m_{\bar{\nu}}^2 = (p_{B_{\text{recoil}}} - p_{D^*} - p_{\ell})^2 < -3(\text{GeV}/c^2)^2$. This selection removes about 68% of the $\bar{B}^0 \rightarrow D^{*+} \ell^- \bar{\nu}$ background without significantly affecting the signal $\bar{B} \rightarrow X_u \ell \bar{\nu}$ decays.

The detection of kaons in the recoil system is a powerful tool to veto background, since less than $\sim 10\%$ of all $\bar{B} \rightarrow X_u \ell \bar{\nu}$ decays contain kaons, whereas a large fraction of charm particles decay in charged or neutral kaons. Charged kaons are identified by an algorithm based on the DIRC, DCH and the SVT information. $K_S \rightarrow \pi^+ \pi^-$ decays are selected from pairs of oppositely charged tracks that are kinematically constrained to originate from a common vertex, and have an invariant mass consistent with the K_S mass, $0.486 < m_{\pi^+ \pi^-} < 0.510 \text{ GeV}/c^2$.

We finally separate the events into two subsamples, signal enriched and signal depleted sample, depending on the absence or presence of at least one charged or neutral kaon in the recoiling system. The depleted sample is used as a control sample to study in detail that the Monte Carlo simulation reproduces the resolutions accurately.

2.5 Extraction of Branching Ratios

We derive $|V_{ub}|$ from a measurement of the ratio of branching fractions

$$R_{u/sl} = \frac{\mathcal{B}(\bar{B} \rightarrow X_u \ell \bar{\nu})}{\mathcal{B}(\bar{B} \rightarrow X \ell \bar{\nu})} = \frac{N_u / (\varepsilon_{\text{sel}}^u \varepsilon_{m_X}^u)}{N_{sl}} \times \frac{\varepsilon_l^{sl} \varepsilon_t^{sl}}{\varepsilon_l^u \varepsilon_t^u}, \quad (1)$$

observed for the admixture of B^0 and B^+ in the B_{reco} tagged sample.

The denominator $N_{sl} = N_{sl}^{\text{meas}} - BG_{sl}$ is the number of events with at least one charged lepton fulfilling the charge-flavor correlation. N_{sl}^{meas} is derived from a fit to the m_{ES} distribution with the sum of an empirical background function⁷ describing the contribution from both continuum events and combinatorial background from $B\bar{B}$ events and a narrow signal⁸ peaked at the B meson mass. This fit, shown in Figure 1a, results in $N_{sl} = 32210 \pm 230$ events. The residual background BG_{sl} is mainly due to misidentified leptons and semileptonic charm decays; it is estimated by Monte Carlo simulation to be $(6.8 \pm 1.2)\%$ of the total lepton yield.

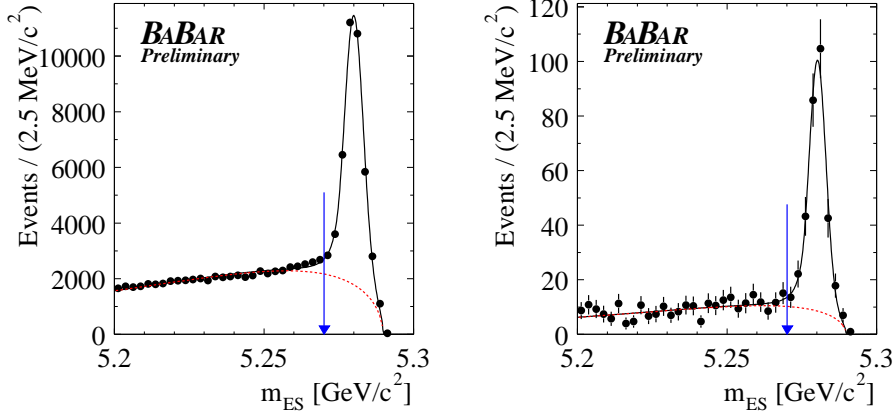


Figure 1: Fit to the m_{ES} distributions for the lepton sample with $p^* > 1 \text{ GeV}/c$ in the recoil of a B_{reco} candidate (left), and for selected events with $m_X < 1.55 \text{ GeV}/c^2$ (right). The arrow indicates the cut on m_{ES} .

The signal yield $N_u^{\text{meas}} = N_u + BG_u$ is determined from events with $m_X < m_X^{\text{cut}}$ in the signal enriched sample (veto on kaons). In each bin of the m_X distribution, the combinatorial B_{reco} background is subtracted based on a fit to the m_{ES} distribution. Figure 1b shows the m_{ES} distribution for the low mass region $m_X < 1.55 \text{ GeV}/c^2$; we require $m_{\text{ES}} > 5.27 \text{ GeV}/c^2$.

The number of signal events N_u is extracted from a binned χ^2 fit of the measured m_X distribution to the sum of three contributions: the signal, the background from $\bar{B} \rightarrow X_c \ell \bar{\nu}$, and the background from other sources (misidentified leptons, secondary τ and charm decays). The shape of the signal and background contributions are derived from Monte Carlo simulation and their relative normalizations are free parameters in the fit. The χ^2 function takes into account the statistical errors from the m_{ES} fit and from the Monte Carlo sample. Figure 2 shows the m_X distribution (corrected for B_{reco} background) for the $b \rightarrow u$ enriched sample. Also shown are the results of the fit, with the fitted signal and the two background distributions. The fit reproduces the data well, $\chi^2/\text{dof} = 0.85$.

The following efficiency corrections have been determined from Monte Carlo simulations: $\varepsilon_{\text{sel}}^u$ is the efficiency for selecting $\bar{B} \rightarrow X_u \ell \bar{\nu}$ decays with all analysis requirements and is found to be $\varepsilon_{\text{sel}}^u = 0.342 \pm 0.006(\text{stat})$. $\varepsilon_{m_X}^u$ is the efficiency of the cut m_X^{cut} and depends on the theoretical parameters of the Fermi motion. For $m_X^{\text{cut}} = 1.55 \text{ GeV}/c^2$, we obtain $\varepsilon_{m_X}^u = 0.733 \pm 0.009(\text{stat})$.

The following ratios are determined from Monte Carlo simulations: the factor $\varepsilon_l^s/\varepsilon_l^u$ corrects for the difference of the impact of the lepton momentum cut for $\bar{B} \rightarrow X \ell \bar{\nu}$ and $\bar{B} \rightarrow X_u \ell \bar{\nu}$ decays. We estimate for electrons $\varepsilon_e^s/\varepsilon_e^u = 0.896 \pm 0.009$, for muons $\varepsilon_\mu^s/\varepsilon_\mu^u = 0.875 \pm 0.015$, and for the combined sample $\varepsilon_\ell^s/\varepsilon_\ell^u = 0.887 \pm 0.008$. The ratio $\varepsilon_t^s/\varepsilon_t^u$ accounts for a possible difference in the efficiencies for finding a B_{reco} decay in events with semileptonic decays in the recoiling B , $\bar{B} \rightarrow X \ell \bar{\nu}$ and $\bar{B} \rightarrow X_u \ell \bar{\nu}$. This ratio is expected to be close to one. Based on Monte Carlo simulations, we find $\varepsilon_t^s/\varepsilon_t^u = 0.98 \pm 0.04$. We thus assume $\varepsilon_t^s/\varepsilon_t^u = 1.00 \pm 0.04$ and take the statistical error of the Monte Carlo simulation as systematic error.

With these corrections, we obtain for the ratio of branching fractions

$$R_{u/sl} = \frac{\mathcal{B}(\bar{B} \rightarrow X_u \ell \bar{\nu})}{\mathcal{B}(\bar{B} \rightarrow X \ell \bar{\nu})} = 0.0197 \pm 0.0025(\text{stat}) \pm 0.0010(\text{MC stat}) \quad (2)$$

We performed the measurement on various subsamples of data. For B^0 we measure $R_{u/sl} = 0.0246 \pm 0.0043(\text{stat})$ and for B^+ we obtain $R_{u/sl} = 0.0168 \pm 0.0030(\text{stat})$. The result is also stable for different choices of m_X^{cut} , resulting in widely varying signal/background ratios.

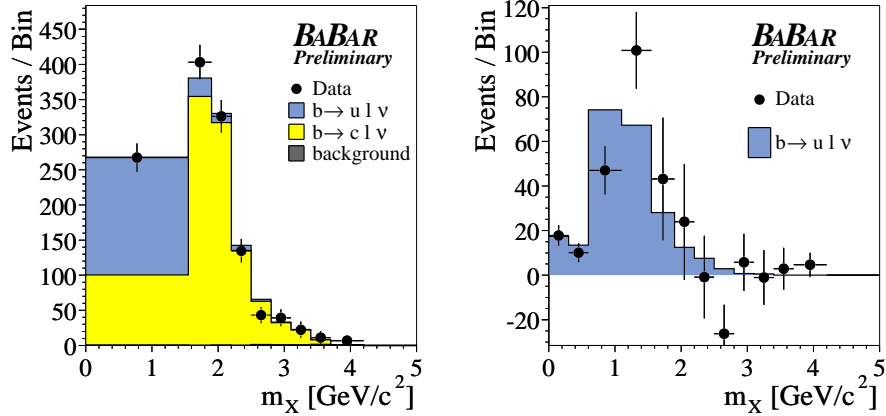


Figure 2: A χ^2 fit to the m_X distribution for the $\bar{B} \rightarrow X_u \ell \bar{\nu}$ enriched sample. Left: the data (points) and three fitted contributions. Right: background subtracted data and signal MC.

2.6 Systematic Uncertainties

Extensive studies have been performed to assess the systematic uncertainties and potential biases that might impact the measurement of $R_{u/sl}$.

The reconstruction of the invariant mass of the hadronic recoil is affected by missing and fake particles, as well as resolution effects. Taking into account the uncertainties related to the reconstruction of charged tracks and neutral particles (including the uncertainty in the energy deposition of K_L in the calorimeter) and to particle identification by the usage of independent control samples we get a relative systematics uncertainty on the branching ratio of 7.5%.

The uncertainty of the B_{reco} combinatorial background subtraction is estimated by changing the signal shape function to a Gaussian and by varying the parameters within one standard deviation of the default values. The binning systematics have been studied by varying the binning for $m_X > 1.55 \text{ GeV}/c^2$. The resulting systematics uncertainty is 6.2%.

While the total semileptonic branching fraction $\bar{B} \rightarrow X \ell \bar{\nu}$ is well measured, the decomposition to individual charm states is much less certain. The impact on $R_{u/sl}$ has been estimated by varying each of the exclusive branching ratios within one standard deviation of the current world average⁴. Similarly, the branching ratios of charm mesons have been varied, both for exclusive decays and for inclusive kaon production. The variation on the branching ratio is 4.4%.

The signal detection efficiency ε_{sel}^u depends on event selection criteria, the composition and average mass of the hadron system and the decay of the final state particles. We study the impact of signal events with two kaons by including events with an even number of kaons in the signal enriched sample. The uncertainty in the hadronization of the final state of $\bar{B} \rightarrow X_u \ell \bar{\nu}$ events is determined by measuring $R_{u/sl}$ in bins of charged and neutral multiplicities. The result agrees well with the standard fit, the difference is smaller than 1%. In addition, we perform the fit using only the non-resonant signal model instead of the hybrid model. The difference to the default method is 3%, which we take as an estimate of the systematic error for the hadronization uncertainties. We vary the inclusive and exclusive branching fractions for the charmless semileptonic B -decays by one standard deviation. The fraction of $s\bar{s}$ popping events is varied by 100% in the exclusive signal contribution and by 30% in the inclusive one. In summary the uncertainty on the $\bar{B} \rightarrow X_u \ell \bar{\nu}$ modeling gives a systematic effect of 4.1%.

Due to the large difference in the reconstruction efficiency for charged and neutral B_{reco} candidates, the event sample contains substantially more B^+ than B^0 mesons. This has a negligible impact on the extraction of the charmless semileptonic branching fraction and $|V_{ub}|$. No correction is applied.

The fraction ε_{m_X} of signal events with $m_X < 1.55 \text{ GeV}/c^2$ is taken from a theoretical calculation of the shape of the hadronic recoil mass distribution and depends on non-perturbative parameters: $\overline{\Lambda} = 0.480 \pm 0.122 \text{ GeV}$ and $\lambda_1 = -0.300 \pm 0.105 \text{ GeV}^2$, where we have taken the recent measurement of CLEO⁹. In the determination of the theoretical error, we use a correlation of -0.8 between the $\overline{\Lambda}$ and λ_1 . The resulting systematic uncertainty is 17.5%.

2.7 Extraction of $|V_{ub}|$

Combining the measured ratio $R_{u/sl}$ with the inclusive semileptonic branching fraction of $\mathcal{B}(\overline{B} \rightarrow X \ell \bar{\nu}) = (10.87 \pm 0.18(\text{stat}) \pm 0.30(\text{syst}))\%$ as determined by *BABAR*¹⁰, we obtain

$$\mathcal{B}(\overline{B} \rightarrow X_u \ell \bar{\nu}) = (2.14 \pm 0.29(\text{stat}) \pm 0.26(\text{syst}) \pm 0.37(\overline{\Lambda}, \lambda_1)) \times 10^{-3}, \quad (3)$$

where we have included the statistical and systematic error of the branching fraction $\mathcal{B}(\overline{B} \rightarrow X \ell \bar{\nu})$. In the context of the OPE, this result translates to

$$|V_{ub}| = (4.52 \pm 0.31(\text{stat}) \pm 0.27(\text{syst}) \pm 0.40(\overline{\Lambda}, \lambda_1) \pm 0.09(\text{pert}) \pm 0.24(1/m_b^3)) \times 10^{-3}. \quad (4)$$

where we have used the average B lifetime of $\tau_B = 1.608 \pm 0.016 \text{ ps}$ ⁴.

The first error is the statistical uncertainty, with contributions from data and Monte Carlo, the second one refers to the experimental systematic uncertainty, the third one gives the theoretical uncertainty in the efficiency determination and extrapolation to the full m_X range, and the remaining errors refer to uncertainties in the extraction of $|V_{ub}|$ from the branching ratio.

3 Measurement of the $B^0 \rightarrow D^{*-} \ell^+ \nu_\ell$ Branching Ratio

3.1 Event selection and reconstruction

We select events containing a fully-reconstructed D^{*-} and an identified oppositely-charged electron or muon. The $D^{*-} \ell^+$ pair is then required to pass kinematic cuts that enhance the $B^0 \rightarrow D^{*-} \ell^+ \nu_\ell$ signal. Several control samples are used to characterize most of the backgrounds. We define the following classification of the sources of signal and backgrounds:

1. events with a correctly reconstructed D^* candidate:
 - (a) events that originate from $B\overline{B}$ events with a correctly identified lepton candidate. They can be separated as: **signal** ($B^0 \rightarrow D^{*-} \ell^+ \nu_\ell(n\gamma)$ decays), **correlated-lepton background** (B^0 or $B^\pm \rightarrow D^{*-} X$, $X \rightarrow \ell^+ Y$), **uncorrelated-lepton background** ($B \rightarrow D^{*-} X$ and other $B \rightarrow \ell^+ Y$), **charged B background** ($B^+ \rightarrow D^{*-} \ell^+ \nu_\ell X$), and **neutral B background** ($B^0 \rightarrow D^{*-} \ell^+ \nu_\ell X$),
 - (b) **fake-lepton background**, e.g. $B\overline{B}$ events, with a hadron misidentified as a lepton;
 - (c) **continuum background**, e.g. $c\bar{c} \rightarrow D^{*-} \ell^+ X$;
2. **combinatorial- D^* background**: events with a mis-reconstructed D^{*-} candidate.

Lepton candidates

Electron and muon candidates are selected according to particle identification criteria which are described in detail elsewhere². In addition to those criteria, they are required to have momentum greater than $1.2 \text{ GeV}/c$ in the $\Upsilon(4S)$ rest frame, since this cut significantly reduces the *correlated-lepton* background. A sample enriched in *fake-lepton* background is also selected, where $D^{*-} h^+$ candidates are accepted if the charged track h^+ fails both electron and muon selection criteria looser than those required for lepton candidates, but fulfills all the other requirements. This sample is used to determine the fraction of the *fake-lepton* background.

D^{*-} candidates

D^{*-} candidates are selected in the decay mode $D^{*-} \rightarrow \bar{D}^0\pi^-$. The \bar{D}^0 candidate is reconstructed in the modes $K^+\pi^-$, $K^+\pi^-\pi^+\pi^-$, $K^+\pi^-\pi^0$, and $K_S^0\pi^+\pi^-$. The daughters of the \bar{D}^0 decay are selected according to the following definitions: π^0 candidates are reconstructed from two photons with energy greater than 30 MeV each, an invariant mass between 119.2 and 150.0 MeV/c^2 , and a total energy greater than 200 MeV. The mass of the photon pair is constrained to the π^0 mass and the photon pair is kept as a π^0 candidate if the χ^2 probability of the fit is greater than 1%. K_S^0 candidates are reconstructed from a pair of charged particles with invariant mass within 15 MeV/c^2 of the K_S^0 mass. The pair of tracks is retained as a K_S^0 candidate if the χ^2 probability that the two tracks form a common vertex is greater than 1%. Charged kaon candidates satisfy loose kaon criteria for the $K^+\pi^-$ mode and tighter criteria for the $K^+\pi^-\pi^+\pi^-$ and $K^+\pi^-\pi^0$ modes. For the $K^+\pi^-\pi^0$ and $K_S^0\pi^+\pi^-$ modes, the candidate is retained if the square of the decay amplitude in the Dalitz plot for the three-body candidate, based on measured amplitudes and phases¹¹, is greater than 10% of its maximum value across the Dalitz plot.

\bar{D}^0 candidates are accepted if they have an invariant mass within 17 MeV/c^2 of the \bar{D}^0 mass in the $K^+\pi^-$, $K^+\pi^-\pi^+\pi^-$ and $K_S^0\pi^+\pi^-$ modes, and 34 MeV/c^2 for the $K^+\pi^-\pi^0$ mode. The invariant mass of the daughters is constrained to the \bar{D}^0 mass and the tracks are constrained to a common vertex in a simultaneous fit. The \bar{D}^0 candidate is retained if the χ^2 probability of the fit is greater than 0.1%.

The low-momentum pion candidates for the $D^{*-} \rightarrow \bar{D}^0\pi^-$ decay are selected with total momentum in the laboratory frame less than 450 MeV/c , and momentum transverse to the beam line in the laboratory frame greater than 50 MeV/c . The momentum of the D^{*-} candidate in the $\Upsilon(4S)$ rest frame is required to be between 0.5 and 2.5 GeV/c .

$D^{*-}\ell^+$ candidates

$D^{*-}\ell^+$ candidates are selected if $|\cos \Delta\theta_{\text{thrust}}^*| < 0.85$, where $\Delta\theta_{\text{thrust}}^*$ is the angle between the thrust axis of the $D^{*-}\ell^+$ candidate and the thrust axis of the remaining charged and neutral particles in the event. The distribution of $|\cos \Delta\theta_{\text{thrust}}^*$ is peaked at 1 for jet-like continuum events, and is flat for $B\bar{B}$ events, where the two B mesons decay independently and practically at rest with respect to each other. $D^{*-}\ell^+$ candidates are selected if the χ^2 probability of the fit to a common vertex of the lepton, of the π^- , and of the \bar{D}^0 candidates is greater than 1%.

We define two angular quantities for each $D^{*-}\ell^+$ candidate. The first angle is $\theta_{D^*,\ell}$, the angle between the D^{*-} and lepton in the $\Upsilon(4S)$ rest frame. The signal distribution of $\cos \theta_{D^*,\ell}$ is peaked around -1 since the signal is more likely back-to-back in the $\Upsilon(4S)$ rest frame, while the distribution for the *uncorrelated-lepton* background is flat. A sample enhanced in $B^0 \rightarrow D^{*-}\ell^+\nu_\ell$ signal events (called the *opposite-side* sample) is selected by requiring $\cos \theta_{D^*,\ell} < 0$ while a background control sample, representative of the *uncorrelated-lepton* background (*same-side* sample), is composed of $D^{*-}\ell$ candidates satisfying $\cos \theta_{D^*,\ell} \geq 0$.

The second angle is $\theta_{B^0,D^*\ell}$, the inferred angle between the direction of the B^0 and the vector sum of the D^{*-} and lepton candidate momenta in the $\Upsilon(4S)$ rest frame. Assuming that the only missing particle in the B reconstruction is a neutrino, the cosine of $\theta_{B^0,D^*\ell}$ is calculated using:

$$\cos \theta_{B^0,D^*\ell} = \frac{-(m_{B^0}^2 + m_{D^*\ell}^2 - 2 E_{B^0}^* E_{D^*\ell}^*)}{2 |\vec{p}_{B^0}^*| |\vec{p}_{D^*\ell}^*|}. \quad (5)$$

All quantities in Eq. 5 are defined in the $\Upsilon(4S)$ rest frame. The energy and the magnitude of the momentum of the B are calculated from the e^+e^- center-of-mass energy and the B^0 mass. For true $B^0 \rightarrow D^{*-}\ell^+\nu_\ell$ events, $\cos \theta_{B^0,D^*\ell}$ lies in the physical region $[-1, +1]$, except for detector resolution and beam energy uncertainty. Backgrounds lie inside and outside the range $[-1, +1]$. In particular we use this variable to extract the $B \rightarrow D^{*-}\ell^+\nu_\ell X$ background. Due to missing

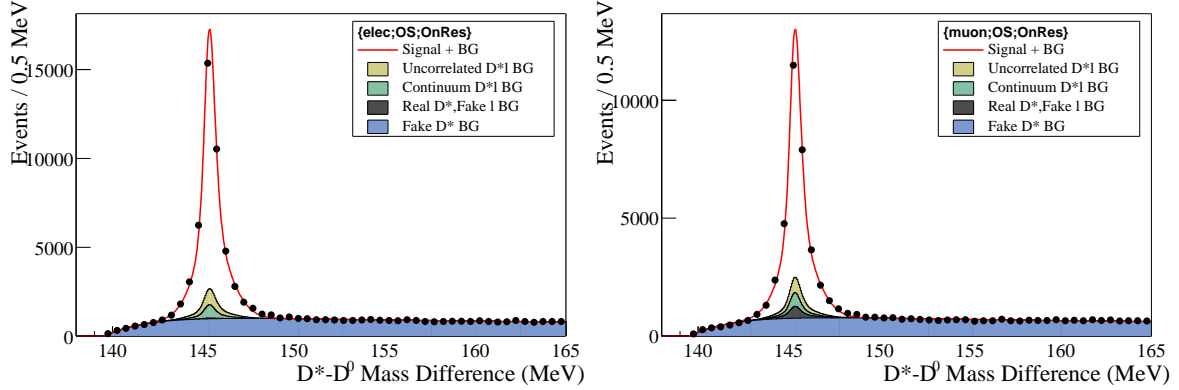


Figure 3: δm distribution for events passing all selection criteria for $B^0 \rightarrow D^{*-} \ell^+ \nu_\ell$ candidates, with (left) an electron or (right) a muon candidate. The points correspond to the data. The curve is the result of a simultaneous unbinned maximum likelihood fit to this sample of events and a number of background control samples. The *correlated-lepton* and $B \rightarrow D^{*-} \ell^+ \nu_\ell X$ backgrounds are included in the signal distribution.

particles not accounted for when evaluating $\cos \theta_{B^0, D^* \ell}$ for such a background event, the result will be less than the true value and it can fall well below the physical region. We use this distribution to perform a χ^2 binned fit for the $B \rightarrow D^{*-} \ell^+ \nu_\ell X$ background fraction.

3.2 Signal extraction

The candidates that pass the above selection criteria are distributed over two signal samples and ten background control samples defined by the following characteristics:

1. whether the data were recorded *on* or *off* the $\Upsilon(4S)$ resonance;
2. whether the candidate lepton is *same-side* or *opposite-side* to the D^{*-} candidate;
3. whether the lepton candidate passes the criteria for an electron, a muon, or a fake lepton.

The ten background samples are used to determine the background levels contaminating the two signal samples.

The *combinatorial-D** background can be distinguished from events with a D^{*-} by means of the mass difference $\delta m = m_{D^*} - m_{D^0}$. Each of the 12 samples described above is divided into 6 subsamples according to the following characteristics that affect the δm distributions.

1. the π^- from the D^{*-} decay is reconstructed in the SVT only, or in the SVT and DCH (two choices): the δm resolution is worse when the π^- is reconstructed only in the SVT.
2. the \bar{D}^0 candidate is reconstructed in the mode $K^+ \pi^-$ or $K^+ \pi^- \pi^0$ or $(K^+ \pi^- \pi^+ \pi^-$ or $K_S^0 \pi^+ \pi^-)$ (three choices): the level of contamination from *combinatorial-D** background and the δm resolution depend on the \bar{D}^0 decay mode.

We fit the δm distributions for each of the total 72 subsamples. The shape of the peak due to real D^{*-} decays is modeled by the sum of two Gaussian distributions; the mean and the variance of the Gaussian distributions and the relative normalization are free parameters. The shape of the *combinatorial-D** background is modeled with

$$\frac{1}{N} \left[1 - \exp \left(-\frac{\delta m - m_{\pi^-}}{c_1} \right) \right] \left(\frac{\delta m}{m_{\pi^-}} \right)^{c_2}, \quad (6)$$

where N is a normalization constant, m_{π^-} is the mass of the π^- , and c_1 and c_2 are free parameters.

We perform a simultaneous unbinned maximum likelihood fit to the 72 δm distributions to obtain the contributions of signal and background. The δm fits for the two signal samples (*opposite-side* $D^{*-} e^+$ and $D^{*-} \mu^+$ candidates in *on-resonance* data) are shown in Fig. 3.

3.3 Determination of systematic errors

One of the largest systematic errors, a relative 2.7%, comes from uncertainties on $\mathcal{B}(\Upsilon(4S) \rightarrow B^0 \bar{B}^0)$; we use $\mathcal{B}(\Upsilon(4S) \rightarrow B^+ B^-)/\mathcal{B}(\Upsilon(4S) \rightarrow B^0 \bar{B}^0) = 1.055 \pm 0.055^a$. The data/Monte Carlo tracking efficiency difference (including both π^0 and K_S^0 identification efficiency, but not the slow pion coming from $D^{*-} \rightarrow \bar{D}^0 \pi^-$ decay) give a 2.7% relative systematic error. The uncertainties on $\mathcal{B}(\bar{D}^0)^4$ account for a relative 2.0% error on $\mathcal{B}(B^0 \rightarrow D^{*-} \ell^+ \nu_\ell)$. The systematic error associated with the uncertainty in the relative composition of the $B \rightarrow D^{*-} \ell^+ \nu_\ell X$ background accounts for a relative 2.0% error. The systematic error coming from data/Monte Carlo reconstruction efficiency differences for the slow pion coming from $D^{*-} \rightarrow \bar{D}^0 \pi^-$ decay accounts for a relative 1.9%. An estimate of the systematic error coming from the acceptance dependence on the HQET form factors has been evaluated by varying the HQET Monte Carlo simulation input parameters within one standard deviation of the measured values¹², giving a relative error of 1.8%. The systematic error coming from the uncertainty on the number of $\Upsilon(4S)$ events accounts for a relative 1.1%. All other systematic errors amount individually to less than a 1% relative error.

3.4 Results

After combining the results for each of the eight signal channels we obtain:

$$\mathcal{B}(B^0 \rightarrow D^{*-} \ell^+ \nu_\ell) = (4.82 \pm 0.03 \pm 0.02 \pm 0.24 \pm 0.17) \text{ \%}.$$

The first error comes from data statistics, the second from Monte Carlo statistics, the third is the systematic error not related to PDG uncertainties, and the last one is the uncertainty due to the errors on PDG branching fractions for $\Upsilon(4S)$, D^{*-} , and \bar{D}^0 exclusive decays.

4 Measurement of Δm_d and τ_{B^0} with exclusively reconstructed $B^0 \rightarrow D^{*-} \ell^+ \nu_\ell$ decays

This analysis¹³ is based on a reduced sample of 23 million $B\bar{B}$ pairs recorded in the years 1999-2000 by BaBar. One of the two B mesons is reconstructed in $B^0 \rightarrow D^{*-} \ell^+ \nu_\ell$ (using the same technique described in the previous chapter), and the charge of the final-state particles identifies the flavor of the B . All the charged tracks in the event, except the reconstructed tracks from the $D^{*-} \ell^+$ pair, are used to identify the flavor of the other B (referred to as B_{tag}). There are five types of tagging categories. The first two tagging categories rely on the presence of a prompt lepton or charged kaons in the event, whose charge is correlated with the b -flavor of the decaying B . The other three categories exploit a variety of inputs (e.g. slow pions, momentum of the track with the maximum center-of-mass momentum) with a neural network technique.

The difference Δt between the two B decay times is determined from the measured separation $\Delta z = z_{D^*l} - z_{tag}$ along the beam axis between the $D^{*-} \ell^+$ vertex and the B_{tag} vertex. The measured Δz is converted into Δt with the known $\Upsilon(4S)$ boost according to the relation $\Delta z = c\beta\gamma\Delta t$ which neglects the small B momentum in the $\Upsilon(4S)$ frame. The resolution on the $D^{*-} \ell^+$ vertex is about 70 μm while the resolution on the B_{tag} vertex is about 160 μm .

The oscillation frequency Δm_d and the lifetime τ_{B^0} are determined simultaneously with an unbinned maximum likelihood fit to the measured Δt distribution. Note that other mixing measurements fix τ_{B^0} to the world average and this is the source of the dominant systematic error. Also the resolution, the fraction of charged B , the mistag and the background parameters are floated in the fit. The results are: $\Delta m_d = 0.492 \pm 0.018(\text{stat}) \pm 0.013(\text{syst}) \text{ ps}^{-1}$ and $\tau_{B^0} = 1.523^{+0.024}_{-0.023}(\text{stat}) \pm 0.022(\text{syst}) \text{ ps}$. The correlation between Δm_d and τ_{B^0} is -0.22. A correction is applied to both Δm_d and τ_{B^0} which takes into account selection and fit biases. The uncertainty

^aThis value has been obtained correcting the average $\mathcal{B}(\Upsilon(4S) \rightarrow B^+ B^-)/\mathcal{B}(\Upsilon(4S) \rightarrow B^0 \bar{B}^0) = 1.072 \pm 0.058^4$ for the lifetime ratio $\tau_{B^+}/\tau_{B^0} = 1.083 \pm 0.017^4$.

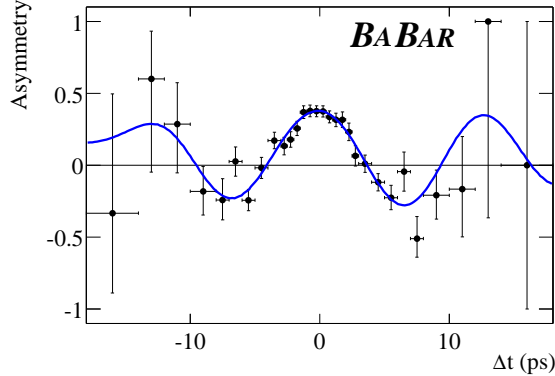


Figure 4: The asymmetry plot for mixed and unmixed events in an 80%-pure signal sample and the projection of the fit results.

on such a correction is the dominant systematic error. Other BaBar measurements for Δm_d and τ_{B^0} can be found in ¹⁴, ¹⁵, ¹⁶ and ¹⁷. Figure 4 shows the mixing asymmetry defined as the difference between the number of unmixed and mixed events over their sum as a function of Δt .

5 Conclusions

We measured the CKM parameter $|V_{ub}| = (4.52 \pm 0.31(stat) \pm 0.27(syst) \pm 0.40(\overline{A}, \lambda_1) \pm 0.09(pert) \pm 0.24(1/m_b^3)) \times 10^{-3}$ using a novel technique based on the study of inclusive semileptonic decays on the recoil of fully reconstructed B mesons. This approach has a smaller systematic uncertainty and higher purity than previous measurements. We also measured the exclusive $B^0 \rightarrow D^{*-} \ell^+ \nu_\ell$ branching ratio $\mathcal{B}(B^0 \rightarrow D^{*-} \ell^+ \nu_\ell) = (4.82 \pm 0.03 \pm 0.02 \pm 0.24 \pm 0.17) \%$. This sample will allow us to extract the $|V_{cb}|$ parameter by studying its differential decay rate. $B^0 \rightarrow D^{*-} \ell^+ \nu_\ell$ events have been also used to measure simultaneously Δm_d and τ_{B^0} .

References

1. N. Cabibbo, Phys. Rev. Lett. **10**, 531 (1963);
M. Kobayashi and T. Maskawa, Prog. Th. Phys. **49**, 652 (1973).
2. B.Aubert *et al.* [BABAR Collaboration], Nucl. Instrum. Meth. A **479**, 1 (2002).
3. D. Scora and N. Isgur, Phys. Rev. D **52**, 2783 (1995).
4. K. Hagiwara *et al.* [Particle Data Group Collaboration], Phys. Rev. D **66**, 010001 (2002).
5. F. De Fazio and M. Neubert, JHEP **9906**, 017 (1999).
6. T. Sjöstrand, Comput. Phys. Commun. **82**, 74 (1994).
7. H. Albrecht *et al.* [ARGUS Collaboration], Z. Phys. C **48**, 543 (1990).
8. T. Skwarnicki [Crystal Ball Collaboration], DESY F31-86-02.
9. D. Cronin-Hennessy *et al.* [CLEO Collaboration], Phys. Rev. Lett. **87**:251808, 2001.
10. B.Aubert *et al.* [BABAR Collaboration], Phys. Rev. D **67**, 031101 (2003).
11. P. L. Frabetti *et al.* [E687 Collaboration], Phys. Lett. B **331**, 217 (1994).
12. CLEO Collaboration, J. Duboscq *et al.*, Phys. Rev. Lett. **76**, 3898 (1996).
13. B.Aubert *et al.* [BABAR Collaboration], Phys. Rev. Lett. **67**, 072002 (2003).
14. B.Aubert *et al.* [BABAR Collaboration], Phys. Rev. Lett. **88**, 221802 (2002).
15. B.Aubert *et al.* [BABAR Collaboration], Phys. Rev. Lett. **88**, 221803 (2002).
16. B.Aubert *et al.* [BABAR Collaboration], Phys. Rev. Lett. **89**, 011802 (2002).
17. B.Aubert *et al.* [BABAR Collaboration], Phys. Rev. Lett. **87**, 201803 (2001).